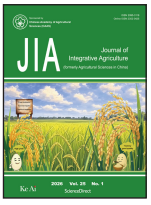
Journal of Integrative Agriculture 2026, 25(1): 127–137

Available online at ScienceDirect

Journal of Integrative Agriculture



RESEARCH ARTICLE

MdXTH30, an apple gene encoding endotransferase/hydrolase for xyloglucan, enhances plant resistance to drought, salt and pathogenic stresses

Shuo Ma, Tong Li, Ziquan Feng, Yali Zhang, Han Jiang#, Yuanyuan Li#

National Apple Engineering Technology Research Center/Shandong Collaborative Innovation Center of Fruit & Vegetable Quality and Efficient Production, College of Horticulture Science and Engineering, Shandong Agricultural University, Tai'an 271018, China

Highlights

- The apple *MdXTH30* could enhance the resistance to drought, salt, and pathogenic bacteria in plants.
- The function of *MdXTH3*0 depends partially on the lignin synthesis mediated by xyloglucan endotransglycosylase/hydrolase.

Abstract

Xyloglucan represents the primary hemicellulose component in higher plant cell walls, providing mechanical support. The XTH gene family encodes xyloglucan endotransferase/hydrolase, a crucial enzyme in cell wall remodeling. Studies examining XTH family-related genes in apples remain limited. This study investigated the *MdXTH30* gene, isolated from apple (*Malus×domestica*), which demonstrated responsiveness to abscisic acid, NaCl, and polyethylene glycol (PEG) 6000, with cytoplasmic localization confirmed through subcellular mapping. To elucidate the role of *MdXTH30* in stress response, transgenic *MdXTH30* apple calli were generated and the gene was heterologously expressed in *Arabidopsis via Agrobacterium*-mediated transformation. The findings revealed that *MdXTH30* enhanced resistance to drought, salt stress, and pathogens through regulation of relevant genes in both apple calli and *Arabidopsis*. These results identify potentially significant candidate genes for improving biotic and abiotic stress resistance at the cell wall level.

Keywords: apple, *MdXTH30*, abscisic acid (ABA) sensitivity, stress resistance

1. Introduction

The cell wall comprises cellulose, hemicellulose, and polysaccharide polymers generated from fruits, serving as the outermost protective layer of plant cells (Zhang B *et al.* 2021). The cell wall facilitates remodeling and enhanced resilience to biotic and abiotic challenges while maintaining cellular integrity, supporting structure, and promoting plant growth (Le Gall *et al.* 2015; Li *et al.* 2019; Zhai *et al.* 2021). The xyloglucan endotransglycosylase/hydrolase (XTH) enzymes, belonging to the glycoside hydrolase 16 (GH16) family, play a crucial role in cell wall remodeling (Henrissat and Davies 1997). Xylodextran hydrolase (XEH) and xylodextran transglycosylase (XET) exemplify XTH proteins. While XEH permanently shortens xylodextran chains, XET facilitates hydrolysis and reformation (Rose *et al.* 2002; Eklöf and Brumer 2010). The xylodextran-specific C-terminal XET domain (C-XET), and the highly conserved glycosylhydrolase family 16 domain (GH16-XET) are also present in the XTH family (Behar *et al.* 2018; Tiika *et al.* 2021). The XTH gene family has been categorized into groups I/II and III based on genetic linkage (Yokoyama *et al.* 2004). Group III subdivides into groups IIIA and IIIB. Members of Group IIIB exhibit transferase activity, whereas those in Group IIIA demonstrate hydrolase activity (Baumann *et al.* 2007). Group III members possess XEH activity, whereas Group I/II enzymes predominantly display XET activity (Bi *et al.* 2024).

XTH plays a vital role in mitigating the effects of biotic and abiotic stressors throughout plant growth and development. The osmotic tolerance of yeast cells in *Populus* increases through heterologous expression of *PtoXTH27/34* (Jiang *et al.*

Received 8 December 2024; Received in revised form 12 March 2025; Accepted 17 June 2025; Available online 22 September 2025
Shuo Ma, E-mail: 15554079103@163.com; #Correspondence Yuanyuan Li, E-mail: liyy0912@163.com; Han Jiang, E-mail: jh12307@163.com

© 2026 CAAS. Publishing services by Elsevier B.V. on behalf of KeAi Communications Co. Ltd. This is an open access article under the CC BY-NC-ND license (http://creativecommons.org/licenses/by-nc-nd/4.0/). Peer review under responsibility of Editorial Board of *Journal of Integrative Agriculture*.
doi: 10.1016/j.jia.2025.09.019

2020). Cadmium tolerance in *Boehmeria nivea* improves through overexpression of *BnXTH1*, *BnXTH6*, and *BnXTH15* (Ma *et al.* 2022). *CsXTH* expression alters when aluminum or fluoride is administered to *Camellia sinensis*, modifying the quantity of xylodextran oligosaccharides in the roots, which affects growth and root development (Wu *et al.* 2021). Overexpressing *DkXTH1* in persimmon results in thicker and stronger cell walls, while ectopic expression of *DkXTH1* in *Arabidopsis* enhances resistance to drought, abscisic acid (ABA), and salt stress (Han *et al.* 2017). Transgenic plants expressing *PeXTH* demonstrate higher fresh weight-to-dry weight ratios and increased water content per unit area compared to natural plants. Additionally, the intercellular gaps between mesophyll and palisade parenchyma cells decrease, improving water retention capacity and enhancing salt stress tolerance while reducing salt tissue concentrations (Han *et al.* 2013). The total fluorescence signal (CTCF, cumulative total cell fluorescence) of XTH-Xet5 increases progressively in resistant varieties after PVY inoculation in potatoes, while declining gradually in susceptible forms (Otulak-Kozieł *et al.* 2018).

The ripening and softening stages of apples constitute the primary focus of current XTH research. During the ripening and softening of 'Taishanzaoxia' apple fruits, the expression levels of *XTH1*, *XTH5*, and *XTH9* decrease. Through activation of genes associated with softness, *XTH2* and *XTH10* potentially function as fruit-softening regulators (Zhang *et al.* 2017). Additionally, *MdNAC7-MdWRKY31* binds to proteins to restrict *MdXTH2* expression, thereby delaying fruit softening (Wang *et al.* 2024). *MdXTHB* exhibits markedly elevated expression levels in the soft apple fruit 'Golden Delicious' (Ma *et al.* 2021). However, the specific role and function of XTH in mitigating biotic and abiotic stress in apples remain incompletely understood.

This study reports the successful cloning of *MdXTH30* from the apple genome and generation of transgenic apple calli and *Arabidopsis*. The findings demonstrate that *MdXTH30* enhances drought and salt resistance while providing protection against pathogenic bacterial infections. This research provides novel insights into the role of XTH family genes in response to abiotic stressors and pathogen challenges at the molecular level.

2. Materials and methods

2.1. Plant materials

The experimental materials consisted of 'Royal Gala' apple trees, tissue-cultured 'GL3' apples, 'Orin' apple calli, *Arabidopsis*, and *Nicotiana benthamiana*.

The roots, stems, leaves, flowers, and fruits were obtained from 'Royal Gala' apple trees cultivated at Shandong Agricultural University, China.

The tissue-cultured 'GL3' apples were cultivated in MS medium containing 0.3 mg L^{-1} 6-benzylaminopurine (6-BA), 0.2 mg L^{-1} 3-indoleacetic acid (IAA), 0.5 mg L^{-1} gibberellin A3 (GA3) and 8 g L^{-1} agar. Growth conditions included a 16 h light/8 h dark photoperiod at 26°C with 60% relative humidity. Samples were subsequently treated with 10% polyethylene glycol (PEG) 6000, 100 mmol L^{-1} NaCl or 100 μmol L^{-1} ABA for 0, 1, 3, 6, 12, 24 and 48 h.

The 'Orin' apple calli were maintained on MS medium supplemented with 1.5 mg L^{-1} 2,4-dichlorophenoxyacetic acid (2,4-D), 0.4 mg L^{-1} 6-enzylaminopurine (6-BA), and 8 g L^{-1} agar, under dark conditions at 26°C for 20 d.

Arabidopsis, comprising ecotype Columbia (Col-0) and three overexpressed strains of the *MdXTH30* (*MdXTH30*-OE1, *MdXTH30*-OE2, *MdXTH30*-OE3), were grown at 21°C under 60% humidity and 16 h light/8 h dark photoperiod. Tobacco plants required 25°C, 65–75% relative humidity, and a 10–12 h photoperiod.

2.2. Bioinformatics analysis of *MdXTH30*

The homologous gene *AtXTH30* and analysis of conserved domains in *AtXTH30*, *MdXTH30* were obtained from the NCBI database *(*https://www.ncbi.nlm.nih.gov/). The base pairs (bp) and amino acids (aa) of the *MdXTH30* sequence were retrieved from the apple genome (https://iris.angers.inra.fr/gddh13/index.html). Protein secondary and tertiary structures were predicted using PSIPRED (http://bioinf.cs.ucl.ac.uk/psipred/), SOPMA (https://npsa-prabi.ibcp.fr/cgi-bin/npsa_automat.pl?page=npsa%20_sopma.html), and SWISS-MODEL (https://swissmodel.expasy.org/interactive). The phylogenetic evolutionary tree of *MdXTH30* was constructed using MEGA_64 software. Multiple sequence alignment was performed using ESPript (https://espript.ibcp.fr/ESPript/ESPript/index.php). The promoter *cis*-acting elements of *MdXTH30* were analyzed using PlantCARE (https://bioinformatics.psb.ugent.be/webtools/plantcare/html/) and visualized with TBtools.

2.3. Construction of *MdXTH30*-related expression vector and genetic transformation of apple calli and *Arabidopsis*

The complete sequence of *MdXTH30* was isolated from tissue-cultured 'GL3' apple leaves and ligated into the cloning vector pMD19-T (TaKaRa, Beijing, China). The overexpression vector (*MdXTH30*-PRI) and silencing vector (*MdXTH30*-RNAi) of *MdXTH30* were constructed using *MdXTH30*-pMD19-T as template. The primer sequences are provided in Appendix A. *MdXTH30*-PRI and *MdXTH30*-RNAi were transformed into *Agrobacterium tumefaciens* LBA4404 for subsequent infection of apple calli (Liu *et al.* 2021). Additionally, *MdXTH30*-PRI was introduced into *A. tumefaciens* GV3101 using the inflorescence infection method to generate three lines of heterologously expressed *MdXTH30* in *Arabidopsis* (Zhang C L *et al.* 2021).

2.4. RNA extraction and real-time quantitative qRT-PCR analysis

RNA extraction was conducted using RNA kits (Tiangen Biotech, Beijing, China) for all samples, including apple calli, various apple tissues, and *Arabidopsis* leaves. First-strand cDNA was synthesized using HiScript III Reverse Transcriptase (Vazyme, Nanjing, China). The cDNA served as template for qRT-PCR analysis using UltraSYBR Mixture (Low ROX) (ComWin BiotechCo., Ltd., Beijing, China). The qRT-PCR analysis followed methods described in Zhong

et al. (2020). All qRT-PCR primer sequences are listed in Appendix A. 18s served as the internal reference gene. Data were analyzed using the $2^{-\Delta\Delta Ct}$ method.

2.5. Subcellular localization of *MdXTH30*

The *MdXTH30*-TOPO vector was initially constructed, followed by generation of *MdXTH30*-RFP through LR recombination. The subcellular localization of *MdXTH30* was visualized using laser scanning confocal microscopy (Zeiss LSM 510 META, Jena, Germany) 1–2 d after transient tobacco transformation.

2.6. Apple calli and *Arabidopsis* were treated with NaCl, ABA and PEG 6000

The 'Orin' apple calli grown under standard conditions were cultured on MS, MS+100 mmol L^{-1} NaCl, MS+50 μmol L^{-1} ABA, MS+6% PEG 6000 medium for 15 to 20 d. Fresh weight, malondialdehyde (MDA) content, and relative conductivity were measured during this period. The protocols for MDA and relative electrical conductivity measurements were adapted from (Hu *et al.* 2016).

Arabidopsis seeds were surface-sterilized in a laminar flow hood and plated on 1/2MS medium. The seeds underwent stratification in darkness at 4°C for 2–3 d. Following 4 d of incubation, *Arabidopsis* seedlings were transferred to 1/2MS, 1/2MS+6% PEG 6000, 1/2MS+100 mmol L^{-1} NaCl and 1/2MS+50 μmol L^{-1} ABA media. Root length measurements were performed after 10 d using ImageJ software.

When *Arabidopsis* developed four true leaves, plants were transplanted into 7 cm×7 cm pots containing medium vermiculite. Water content in each pot was maintained consistently for 15 d under saturated conditions. Control group plants were maintained under standard growth conditions, while treatment group seedlings were exposed to either 150 mmol L^{-1} NaCl or drought stress (water withholding), followed by 2 d rehydration after a 25-d drought period. Post-stress analyses included measurements of hydrogen peroxide (H_2O_2) and superoxide anion ($O_2^{-}\cdot$) levels using the Suzhou Keming kit (Keming, Suzhou, China). Chlorophyll and MDA contents were determined using established protocols. For anthocyanin analysis, 0.1 g of *Arabidopsis* rosette leaves were precisely weighed, finely chopped, and transferred to 10 mL anthocyanin extraction solution (95% anhydrous ethanol and 1.5 mol L^{-1} HCl). The mixture was incubated in darkness until complete anthocyanin extraction. Absorbance measurements were taken using a UV spectrophotometer at 530, 620, and 650 nm. Calculations followed the method described by (An *et al.* 2019).

2.7. Toluidine blue (TB) staining, water loss assays and chlorophyll leaching assays

The stems, rosette leaves, and inflorescents of *Arabidopsis* were immersed in 0.05% TB solution at room temperature for 8 h, rinsed three times with ddH_2O, and photographed on black cloth. For water loss assessment, *Arabidopsis* leaves were placed in darkness and weighed at 30-min intervals until 150 min to determine leaf water loss rate. For chlorophyll leaching analysis, rosette leaves (0.1 g) were immersed in 85% anhydrous ethanol solution in darkness, with absorbance measured at 649 and 665 nm using an ultraviolet spectrophotometer at 10, 30, 60, 120, and 180 min intervals. Chlorophyll concentration was calculated according to Xie *et al.* (2022).

2.8. Nitroblue tetrazolium (NBT) and 3,3-diaminobenzidine (DAB) staining methods

The rosette leaves of *Arabidopsis* were immersed in 0.5 mg mL^{-1} NBT dye solution, vacuum-treated for 15 min, incubated at room temperature in darkness for 4 h, boiled in fixation solution (Anhydrous ethanol:Lactic acid:Glycerol=3:1:1) for 5 min, rinsed three times with anhydrous ethanol, and examined for staining results.

The rosette leaves of *Arabidopsis* were immersed in 1 mg mL^{-1} DAB staining solution at pH 3.8 and vacuum-infiltrated for 30 min. Samples were incubated at 28°C in darkness for 6 h, boiled in fixation solution for 5 min for decolorization, and rinsed three times with anhydrous ethanol before observation.

2.9. Pathogen infection test

The 'Orin' apple calli were cultured on MS medium containing 1.5 mg L^{-1} 2,4-D, 0.4 mg L^{-1} 6-BA and maintained for one week in darkness at 26°C. The calli were inoculated with a 0.5 cm diameter AGAR dish containing *Botryosphaeria dothidea* cultured for 5 d in 28°C dark conditions (Gu *et al.* 2021).

The *Pst* DC3000 was cultured overnight in LB liquid medium at 28°C with agitation until reaching an optical density (OD_{600}) of ≥1. The culture was then resuspended in 10 mmol L^{-1} $MgCl_2$ solution to achieve an OD of 0.01. *Arabidopsis* rosette leaves received dorsal injections using a 1 mL needle-free syringe, while control groups received equivalent injections of 10 mmol L^{-1} $MgCl_2$ solution (Tuang *et al.* 2020).

2.10. Data processing and statistical analysis

Each experiment comprised three parallel trials and three technical replicates to ensure experimental accuracy. Statistical analysis was conducted using IBM SPSS statistics, utilizing the single-factor Duncan method.

3. Results

3.1. Bioinformatics analysis of the *MdXTH30* gene

The *MdXTH30* gene (MD16G1278900) was identified in the apple genome through BLAST analysis of *Arabidopsis XTH30* (AT1G32170.1) in the NCBI database. The complete sequence of *MdXTH30* was 1,068 bp and encoded 356 amino acids. A highly conserved domain exists in both *MdXTH30* and *AtXTH30* (Fig. 1-A). Analysis of the *MdXTH30* secondary structure using the PSIPRED website revealed a predicted structure consisting of 3.10% beta turns, 17.46% alpha helices, 54.65% random coils, and 24.79% extended strands (Fig. 1-B; Appendix B). Tertiary structure prediction using the Phyre2 program demonstrated substantial structural overlap between *MdXTH30* and *AtXTH30* (Fig. 1-C).

3.2. Multiple sequence alignment and phylogenetic analysis of XTH30 proteins

To better understand the evolutionary relationships among

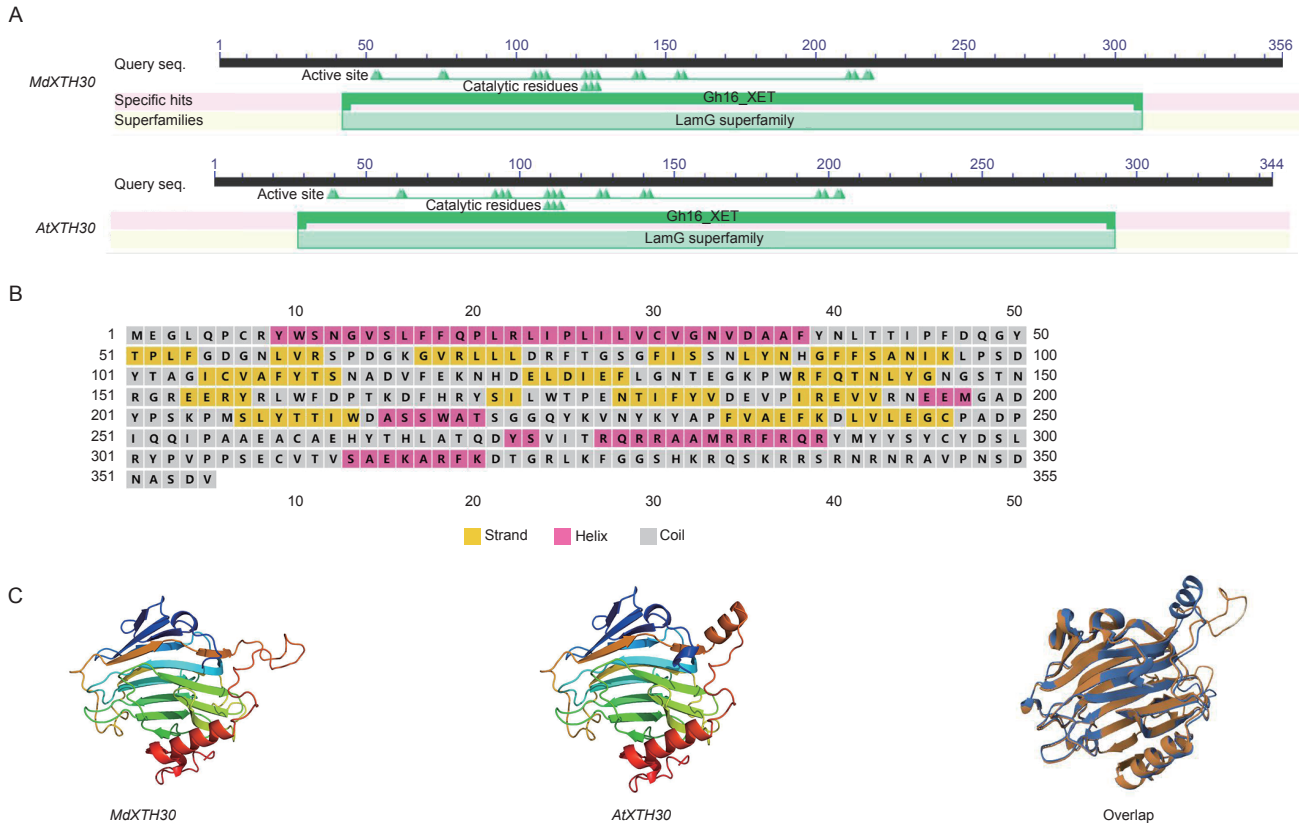


Fig. 1 Analysis of the coding sequence of *MdXTH30*. A, conserved domain analysis of *MdXTH30* and *AtXTH30*. B, predicted protein secondary structure of *MdXTH30*, with different structural elements represented by distinct colors; yellow indicates chain regions, pink indicates helical structures, and gray indicates coiled regions. C, tertiary structure comparison of *MdXTH30* and *AtXTH30* proteins.

XTH30 proteins across species, MEGA_64 software was utilized to analyze 20 XTH30 protein sequences. The phylogenetic analysis revealed that apple *MdXTH30* shared the closest evolutionary relationship with *Pyrus ussuriensis*×*Pyrus communis* (Fig. 2-A). Multiple sequence alignment demonstrated that these species, belonging to the LamG superfamily, contained a highly conserved GH16-XET domain (Fig. 2-B).

3.3. subcellular localization of *MdXTH30*

To determine the cellular localization of the protein, the 35S::*MdXTH30*-RFP vector was constructed. The vector was transiently expressed in tobacco epidermal cells using *A. tumefaciens*. Although *MdPAT16* is known to be localized to the cell membrane, the red fluorescence of *MdXTH30*-RFP did not completely overlap with the green fluorescence of *MdPAT16*-GFP. These observations suggest that this protein may be localized in the cytoplasm (Fig. 3).

3.4. Expression profiles in different apple tissues and expression levels under ABA, NaCl, PEG 6000 of *MdXTH30*

Previous research on pears has demonstrated that the XTH family shows highest expression in stems. To investigate whether *MdXTH30* exhibited similar expression patterns in apple, expression levels were analyzed across multiple tissues, including roots, stems, leaves, flowers, and fruits. The analysis revealed that *MdXTH30* demonstrated the highest expression level in stem tissue and the lowest in leaf tissue (Fig. 4-A).

To elucidate the potential function under abiotic stress, the *cis*-acting elements in the promoter region of *MdXTH30* were analyzed. The analysis indicated responsiveness to ABA, MeJA, auxin, and other hormones, as well as light and low temperatures (Appendix C). Expression levels of *MdXTH30* in ‘Royal Gala’ apple seedlings were measured at various time points following treatment with ABA, NaCl, and PEG 6000.

The expression of *MdXTH30* under ABA treatment reached its maximum at 3 h, followed by a decrease, and subsequently increased again at 24 h (Fig. 4-B). Under NaCl treatment, *MdXTH30* expression showed an initial increase followed by a decrease within 0–6 h, peaked at 12 h, and subsequently declined (Fig. 4-C). During PEG 6000 treatment, *MdXTH30* expression remained relatively stable from 0–3 h, increased at 6 h, subsequently decreased, and reached its peak at 24 h (Fig. 4-D). These expression patterns suggest that *MdXTH30* may play a role in responses to various abiotic stresses.

3.5. *MdXTH30* transcription levels under ABA, NaCl and PEG 6000 treatments

Transgenic apple calli with overexpression of *MdXTH30* (*MdXTH30*-OE) and suppression of *MdXTH30* (*MdXTH30*-RNAi) were generated (Fig. 5-A) to examine the expression

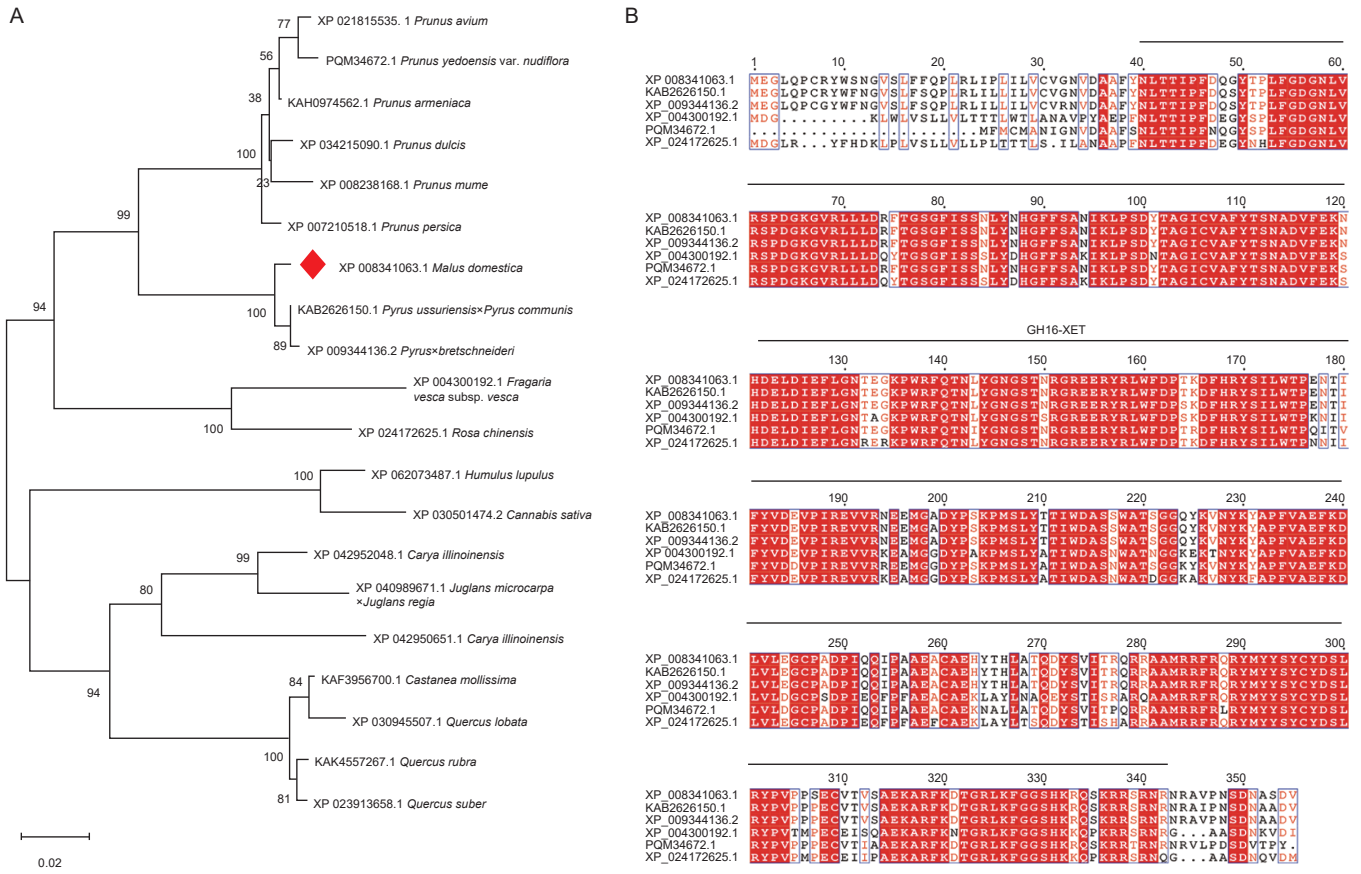


Fig. 2 Phylogenetic relationship and sequence comparison of *MdXTH30*. A, phylogenetic tree constructed from XTH30 proteins of 20 distinct species: *Malus domestica*, *Pyrus ussuriensis*×*Pyrus communis*, *Pyrus*×*bretschneideri*, *Fragaria vesca* subsp. *Vesca*, *Prunus avium*, *Prunus yedoensis* var. *nudiflora*, *Prunus armeniaca*, *Prunus dulcis*, *Prunus mume*, *Prunus persica*, *Humulus lupulus*, *Rosa chinensis*, and *Cannabis sativa*, *Carya illinoinensis*, *Quercus lobala*, *Quercus rubra*, and *Quercus suber*, as well as *Carya illinoinensis*, *Juglans microcarpa*×*Juglans regla* and *Carya illinomensis*. B, multiple sequence alignment of these sequences: *XP 008341063.1*, *KAB2626150.1*, *XP 009344136.2*, *XP 004300192.1*, *PQM34672.1*, *XP 024172625.1*. The black line indicates the conserved domain GH16-XET.

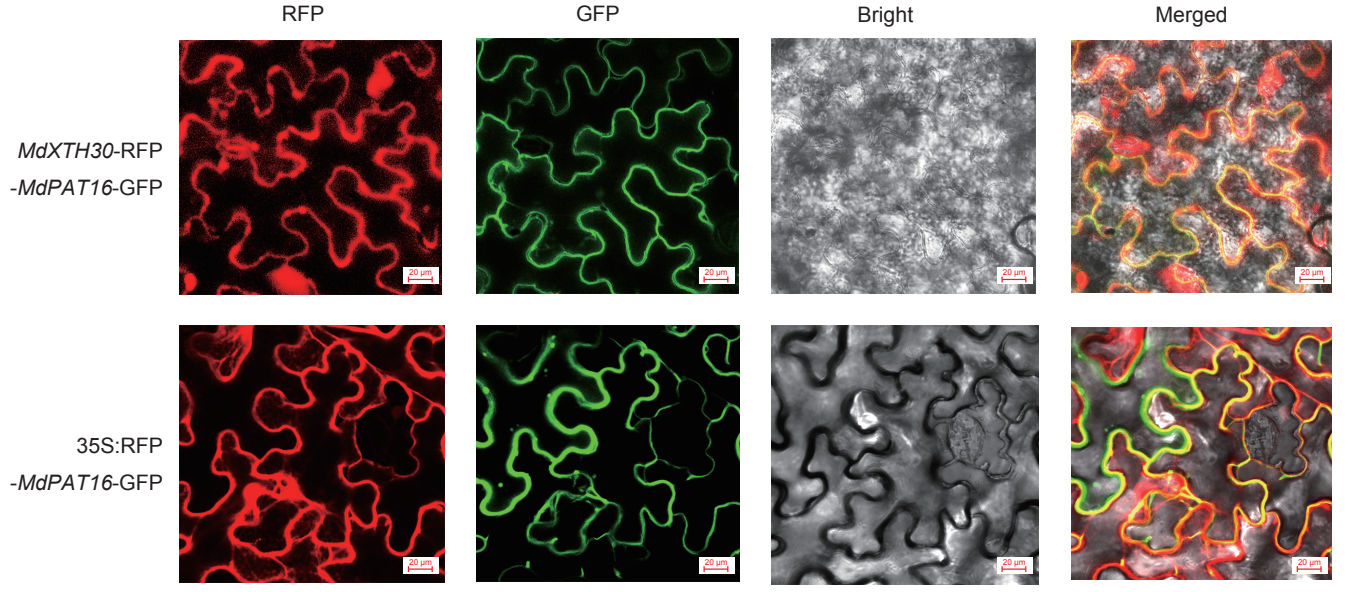


Fig. 3 Subcellular localization of *MdXTH30*. Subcellular localization of *MdXTH30* in epidermal cells of *Nicotiana benthamiana* (bar=20 μm).

of *MdXTH30* under abiotic stresses in greater detail. Following 15 d of growth in MS medium (Fig. 5-B), no significant difference in fresh weight was observed among the wild type (WT) and the *MdXTH30*-OE, *MdXTH30*-RNAi calli under normal conditions. However, under 50 μmol L^{-1} ABA treatment, the fresh weight of *MdXTH30*-OE calli was lower than that of WT, while *MdXTH30*-RNAi exhibited significantly higher fresh weight than WT. Under 100 mmol L^{-1} NaCl and 6% PEG 6000 treatment, the *MdXTH30*-OE calli demonstrated higher fresh weight compared to WT, whereas *MdXTH30*-RNAi showed the opposite pattern (Fig. 5-C). The MDA content (Fig. 5-D) and relative conductivity (Fig. 5-E) displayed inverse patterns between *MdXTH30* transgenic calli and WT.

Furthermore, analysis of gene expression levels of ABA-related genes (*RD29A*, *NCED3*, *EM6*) and salt-related genes (*SOS3*) in WT and the *MdXTH30*-OE, *MdXTH30*-RNAi apple calli under the aforementioned stress treatments (Appendix D) revealed that, compared to WT, the expression of these genes was upregulated in *MdXTH30*-OE calli and downregulated in *MdXTH30*-RNAi calli. These findings indicate that *MdXTH30* can alleviate oxidative damage

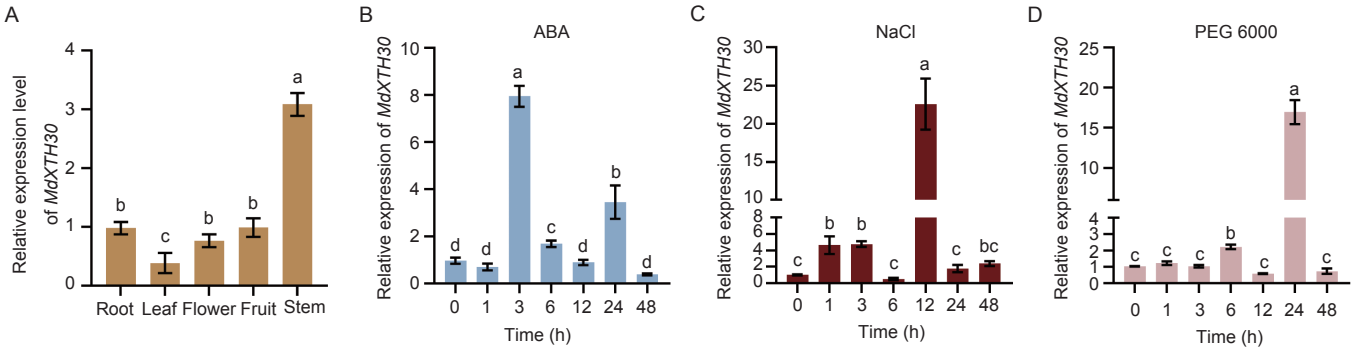


Fig. 4 Expression changes of *MdXTH30* under different conditions. A, expression of *MdXTH30* in different apple tissues measured by RT-qPCR. B–D, relative expression levels of *MdXTH30* under different stress treatments: abscisic acid (ABA) (B), NaCl (C), and PEG 6000 (D) measured by RT-qPCR. Values are mean±SD standard deviation of at least three biological replicates. Different lowercase letters indicate a significant difference at $P<0.05$.

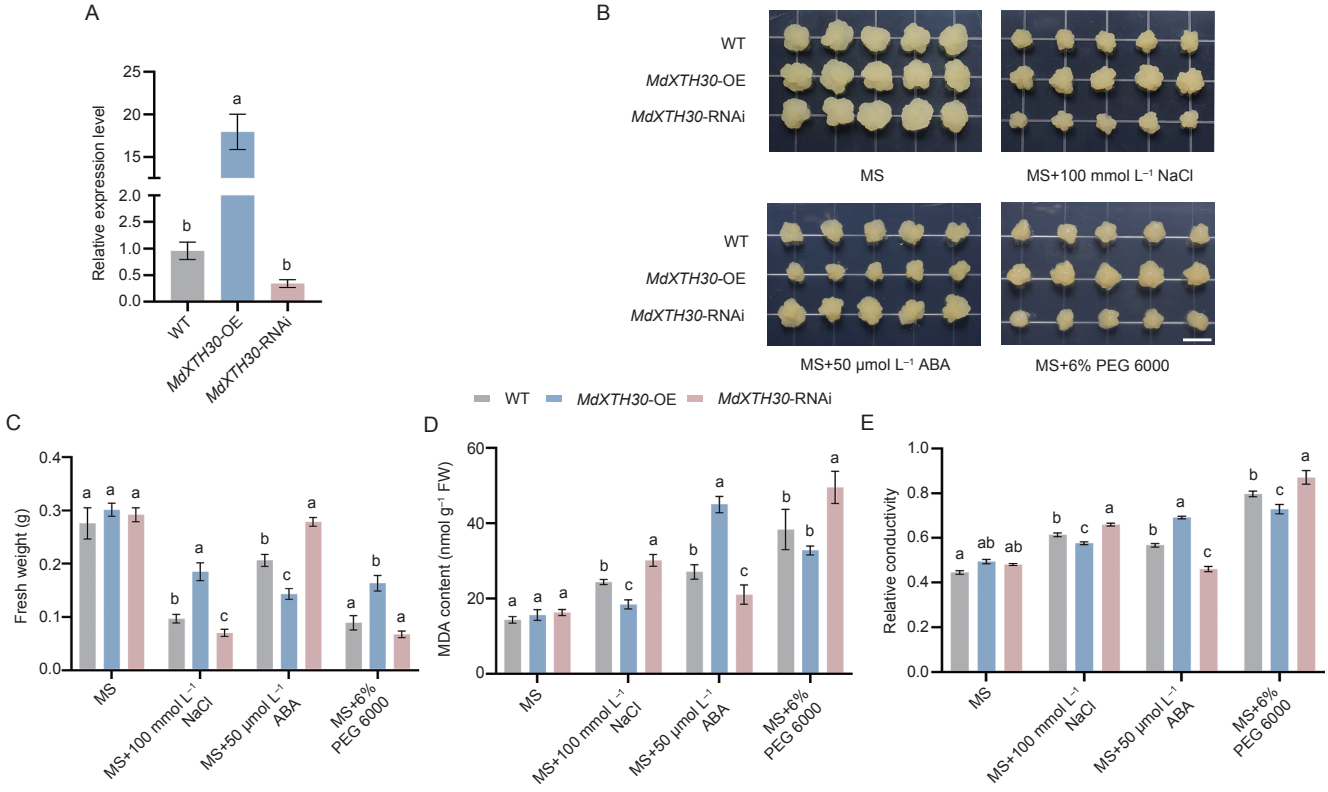


Fig. 5 The overexpression of *MdXTH30* calli enhances resistance to abiotic stress. A, expression of *MdXTH30* in transgenic calli was examined. B, phenotypes of *MdXTH30* transgenic calli and WT in MS, MS+100 mmol L^{-1} NaCl, MS+50 μmol L^{-1} abscisic acid (ABA), MS+6% PEG 6000. C–E, indices of *MdXTH30* transgenic calli and WT under stress treatment: C, fresh weight (FW); D, malondialdehyde (MDA) content; E, relative conductivity. Values represent mean±SD of at least three biological replicates. Different lowercase letters indicate significant differences at $P<0.05$.

under abiotic stress by reducing MDA accumulation and cell membrane permeability.

3.6. Ectopic expression of the apple *MdXTH30* in *Arabidopsis* enhances plant resistance to abiotic stress

To further elucidate the function of *MdXTH30* in response to abiotic stress, we generated the 35S::*MdXTH30*-GFP construct and introduced it into *Agrobacterium*. Ectopically expressed *Arabidopsis MdXTH30* was obtained through inflorescence infiltration (Appendix E). Transgenic *MdXTH30* and Col-0 *Arabidopsis* were cultured on 1/2 MS medium for 3–4 d, then transferred to 1/2 MS medium supplemented with 6% PEG 6000, 100 mmol L^{-1} NaCl, and 50 μmol L^{-1} ABA for approximately 1 week before observations (Fig. 6-A). While no significant difference in root length was observed between *MdXTH30* transgenic plants and Col-0 under normal conditions, under 6% PEG 6000 and 100 mmol L^{-1} NaCl treatments, the roots of *MdXTH30* transgenic *Arabidopsis* were significantly longer than those of Col-0. However, on 50 μmol L^{-1} ABA medium, the roots of *MdXTH30 Arabidopsis* were shorter than those of Col-0 (Fig. 6-B). These results indicate that *MdXTH30* enhances salt stress resistance in *Arabidopsis* and improves drought tolerance through increased ABA sensitivity.

The *MdXTH30* transgenic *Arabidopsis* seedlings were grown under normal conditions for 3 weeks, and then subjected to drought, 150 mmol L^{-1} NaCl, and normal conditions respectively. After 25 d, *Arabidopsis* plants grown under drought or 150 mmol L^{-1} NaCl exhibited reduced growth compared to control conditions (Figs. 7-A and 8-A). However, under stress conditions, *MdXTH30* transgenic *Arabidopsis* demonstrated superior growth compared to Col-0. The chlorophyll content in *MdXTH30* transgenic *Arabidopsis* was elevated relative to Col-0 (Figs. 7-B; 8-B), while the levels of $O_2^{\cdot-}$, H_2O_2, and MDA were reduced (Figs. 7-C and E and 8-C and E).

To evaluate the impact of *MdXTH30* on drought resistance in transgenic plants, Toluidine Blue staining was performed on the inflorescences, stems, and rosette leaves of *Arabidopsis*. The analysis revealed that the stained area and intensity in *MdXTH30* transgenic *Arabidopsis* were significantly reduced compared to Col-0. Furthermore, measurements of leaf water loss rate and chlorophyll leaching rate in wild type and *MdXTH30* transgenic *Arabidopsis* demonstrated that both parameters were significantly lower in *MdXTH30* transgenic lines compared to wild type. These results provide evidence that *MdXTH30* enhances plant drought resistance through reduced epidermal permeability (Appendix E).

3.7. *MdXTH30* enhances plant resistance to pathogens

While the role of XTH family genes in abiotic stress has been extensively studied (Eklöf and Brumer 2010), their function

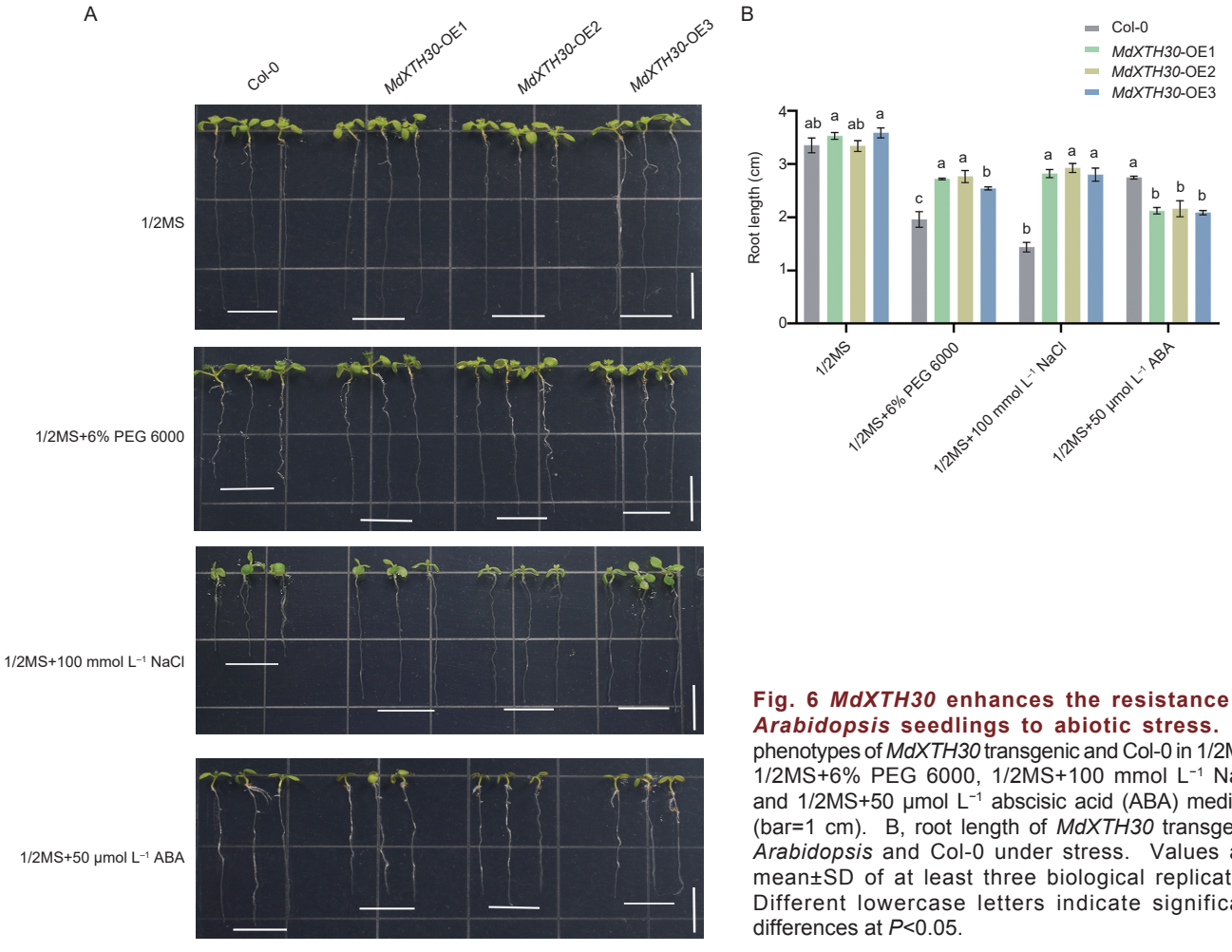


Fig. 6 *MdXTH30* enhances the resistance of *Arabidopsis* seedlings to abiotic stress. A, phenotypes of *MdXTH30* transgenic and Col-0 in 1/2MS, 1/2MS+6% PEG 6000, 1/2MS+100 mmol L^{-1} NaCl and 1/2MS+50 μmol L^{-1} abscisic acid (ABA) medium (bar=1 cm). B, root length of *MdXTH30* transgenic *Arabidopsis* and Col-0 under stress. Values are mean±SD of at least three biological replicates. Different lowercase letters indicate significant differences at $P<0.05$.

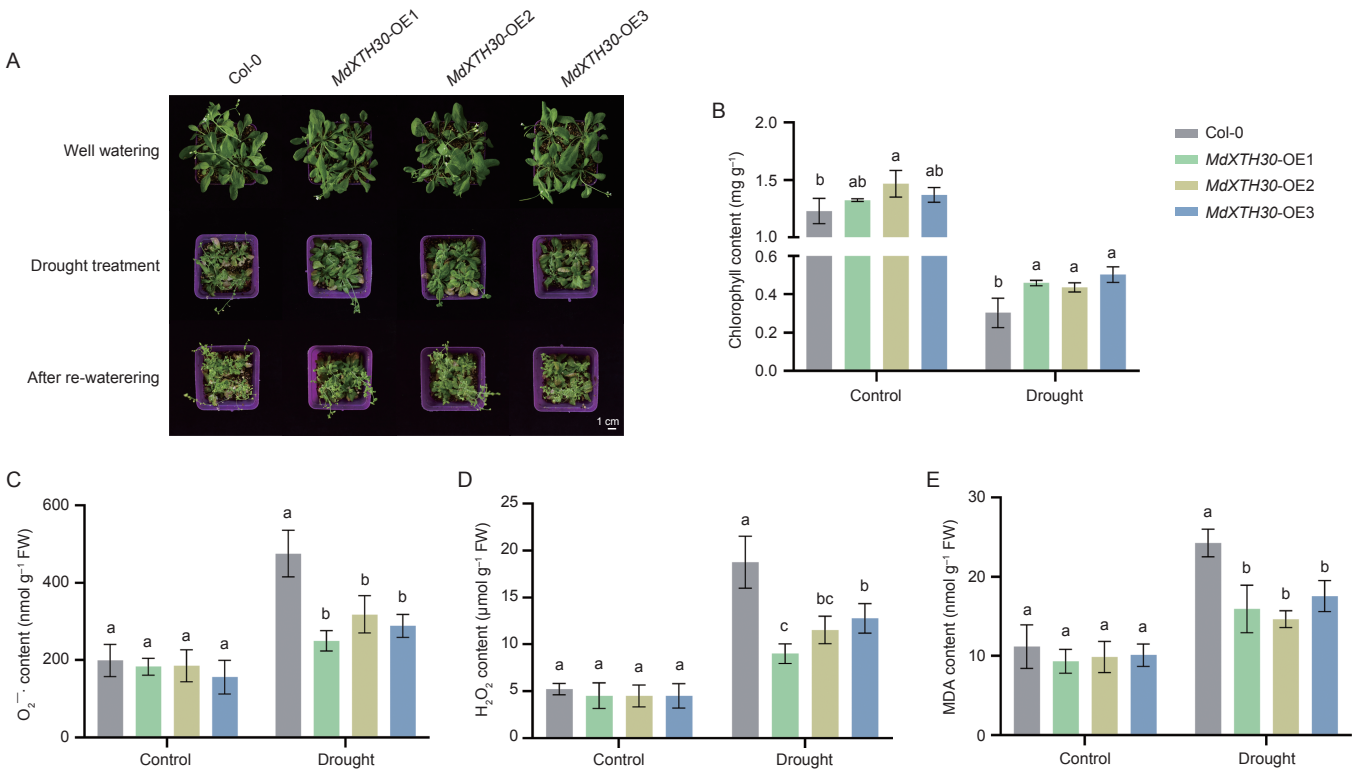


Fig. 7 *MdXTH30* enhanced the resistance of *Arabidopsis* to drought stress. A, phenotypes of *MdXTH30* transgenic *Arabidopsis* and Col-0 under normal conditions and after 25 d of drought, 2 d of re-watering (bar=1 cm). B, chlorophyll content. C, $O_2^{\cdot-}$ content. D, H_2O_2 content. E, malondialdehyde (MDA) content. Values are mean±SD of at least three biological replicates. Different lowercase letters indicate a significant difference at $P<0.05$.

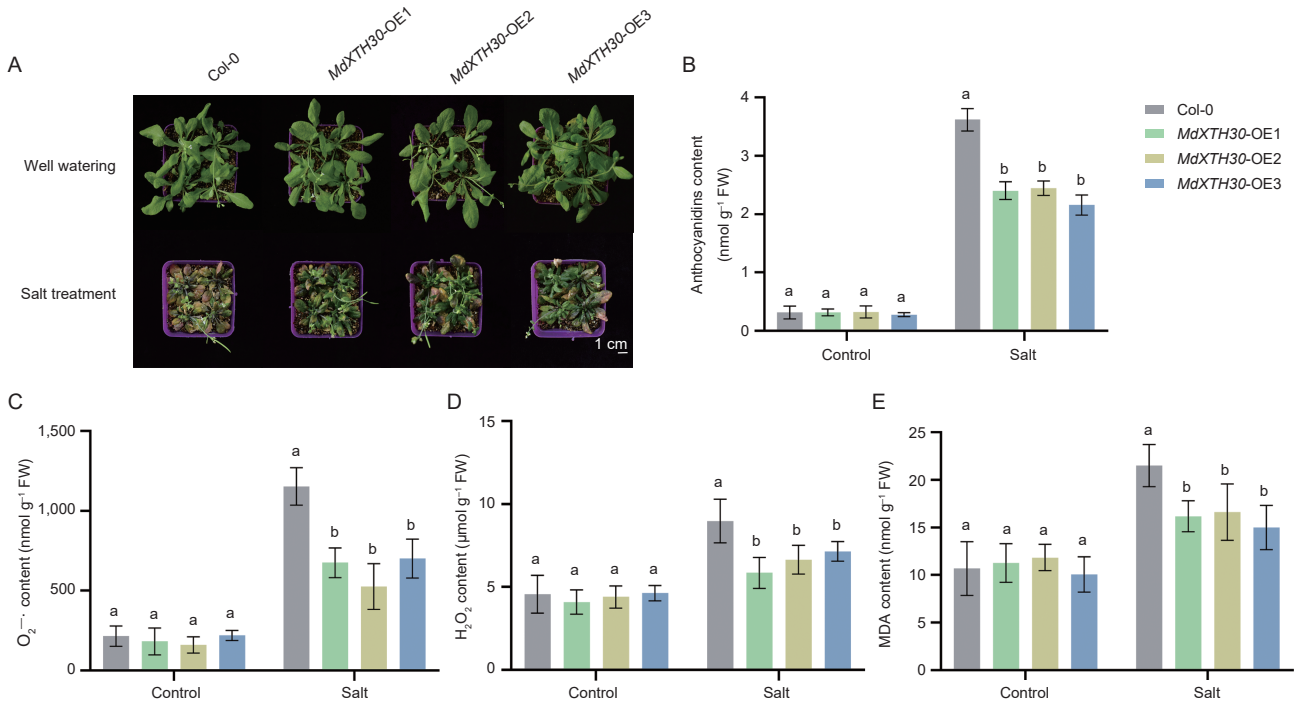


Fig. 8 *MdXTH30* enhanced the resistance of *Arabidopsis* to salt stress. A, phenotypes of *MdXTH30* transgenic *Arabidopsis* and Col-0 under normal conditions and 150 mmol L^{-1} NaCl stress (bar=1 cm). B, anthocyanidins content. C, $O_2^{\cdot-}$ content. D, H_2O_2 content. E, malondialdehyde (MDA) content. Values are mean±SD of at least three biological replicates. Different lowercase letters indicate a significant difference at $P<0.05$.

in response to pathogen stress in apples remains unclear. *MdXTH30*-OE, *MdXTH30*-RNAi, and WT apple calli cultured on MS medium were inoculated with the pathogen *B. dothidea* and incubated at 28°C for 1 week (Fig. 9-A). The infected area on the *MdXTH30*-OE calli was significantly reduced compared to the WT (Fig. 9-B). Following inoculation, H_2O_2 and MDA levels were measured in the calli. H_2O_2 activity was elevated in the *MdXTH30*-OE calli compared to the WT, while MDA content was decreased (Fig. 9-C and D). Analysis of pathogen-related genes (*PR1*, *PR5*, *PAD4*, *PAL*, and *EDS1*) revealed higher expression levels in *MdXTH30*-OE calli compared to WT, whereas expression was reduced in *MdXTH30*-RNAi calli (Fig. 9-E). These findings indicate that *MdXTH30* enhances disease resistance by promoting the expression of pathogen-related genes.

To validate the function of the *MdXTH30* gene in pathogen resistance, *MdXTH30* transgenic *Arabidopsis* and Col-0 were inoculated with *Pst* DC3000 pathogen. The results showed that *MdXTH30* transgenic *Arabidopsis* exhibited reduced leaf blight compared to Col-0 after *Pst* DC3000 pathogen inoculation, while leaf conditions remained comparable between *MdXTH30* transgenic *Arabidopsis* and Col-0 after $MgCl_2$ treatment (Fig. 10-A). Chlorophyll content in *MdXTH30* transgenic *Arabidopsis* leaves exceeded that of Col-0 (Fig. 10-B). NBT and DAB staining revealed that both staining area and intensity were higher in *MdXTH30* transgenic *Arabidopsis* compared to Col-0 (Fig. 10-C–E).

4. Discussion

Environmental stress impedes the progressive improvement of fruit quality (Ngou *et al.* 2022; Li *et al.* 2024). Plants have developed multiple essential mechanisms to cope with stress (Charng *et al.* 2022). However, most studies on regulatory mechanisms have focused on internal regulation, with limited research on external regulatory mechanisms, particularly epidermal regulatory mechanisms.

The GH16-XET domain, highly conserved in the XTH gene family and belonging to glycosyl hydrolase family 16, encodes glycosyltransferase/hydrolase in xyglucan. Research has demonstrated that drought tolerance increases in *Arabidopsis* through overexpression of *TaXTH12.5* in wheat, leading to enhanced germination rates and secondary root development (Han *et al.* 2023). While most research on the XTH family in apples has focused on fruit ripening and softening, studies examining the XTH family's response to abiotic stress remain limited (Muñoz-Bertomeu *et al.* 2013). This study identified the apple gene *MdXTH30*, a characteristic member of the XTH family containing a highly conserved GH16-XET domain. The gene showed peak expression in stems, with protein localization primarily in the cytoplasm. Overexpression of *MdXTH30* enhanced apple resistance to salt and drought stress. The study suggests that *MdXTH30* regulates apple drought tolerance through the ABA pathway, as evidenced by increased ABA sensitivity upon overexpression. Furthermore, *MdXTH30* overexpression enhanced peroxidase

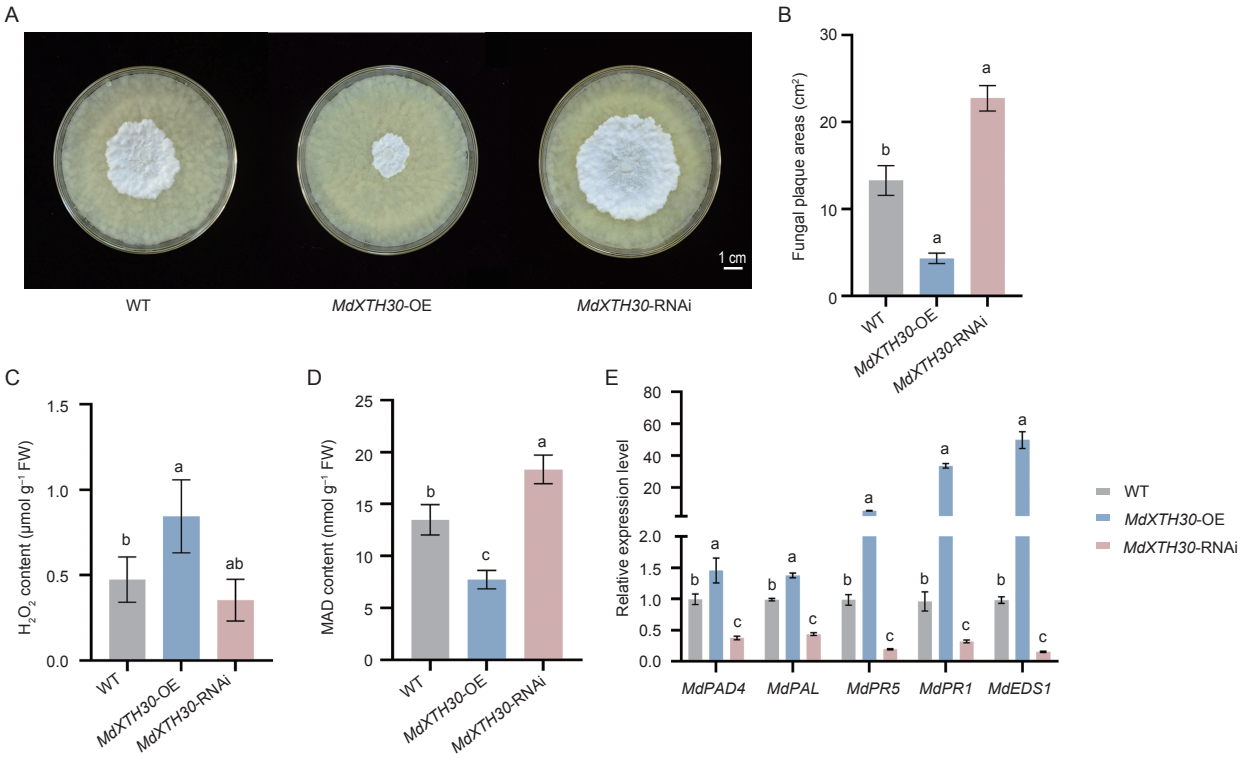


Fig. 9 *MdXTH30* enhances resistance of apple calli to *Botryosphaeria dothidea*. A, phenotypes of *MdXTH30* and WT calli 6 d after inoculation with pathogenic bacteria (bar=1 cm). B, 6 d post-infection, quantitative analysis of fungal patch areas in calli tissue. C, malondialdehyde (MDA) content. D, H_2O_2 content. E, expression changes of disease-resistance related genes in *MdXTH30* and WT calli following inoculation with *B. dothidea*. Values represent mean±SD from at least three biological replicates. Different lowercase letters indicate significant differences at $P<0.05$.

activity and disease resistance, as demonstrated by DAB and NBT staining results (Fig. 10).

Previous research indicates that ethylene upregulates cell wall remodeling genes in mung bean sprouts, including *XTH*, resulting in increased lignin content and enhanced root lignification (Huang *et al.* 2013). The relationship between *XTH* and lignin accumulation in apples remains unexplored. This study found that ectopically expressed *Arabidopsis* and *MdXTH30* overexpressing calli exhibited resistance to salt and drought stress, potentially correlating with lignin accumulation. Additionally, transgenic calli studies revealed that XTH may enhance stress resistance by promoting the expression of internal genes, including *MdRD29A*, *MdSOS3*, MdEM6, and others (Appendix D). These results suggest that *XTH* genes enhance stress resistance through both internal response mechanisms and external gene processes.

In summary, *MdXTH30* demonstrates stress and pathogen resistance capabilities through the activation of pathogen-related and internal stress genes. While *MdXTH30* may confer external stress resistance through lignin accumulation, further research is required. This investigation provides fundamental insights into the XTH family's resistance to external stress and identifies potential candidate genes for enhancing apple lignin synthesis and abiotic stress tolerance.

5. Conclusion

The apple *MdXTH30* gene enhances plant resistance to abiotic stress and pathogen infection.

Acknowledgements

This research was supported by the National Key R&D Plan Project (2023YFD2301000), the National Key Research and Development Program of Shandong Province, China (2024CXGC010903 2023CXPT013), the National Natural Science Foundation of China (32472705, 32302513), the Young Talent of Lifting Engineering for Science and Technology in Shandong, China (SDAST2024QTA083) and the Natural Science Foundation of Shandong Province, China (ZR2022JQ14, ZR2022QC112).

Declaration of competing interest

The authors declare that they have no conflict of interest.

Declaration of generative AI and AI-assisted technologies in the writing process

The authors declare that they did not use AI in the preparation and writing of this manuscript.

Appendices associated with this paper are available at https://doi.org/10.1016/j.jia.2025.09.019

References

An J P, Zhang X W, You C X, Bi S Q, Wang X F, Hao Y J. 2019. *MdWRKY40* promotes wounding-induced anthocyanin biosynthesis in association with *MdMYB1* and undergoes *MdBT2*-mediated degradation. *New Phytologist*, **224**, 380–395.

Baumann M J, Eklöf J M, Michel G, Kallas A s M, Teeri T T, Czjzek M, Brumer H. 2007. Structural evidence for the evolution of xyloglucanase activity from xyloglucan endo-transglycosylases:

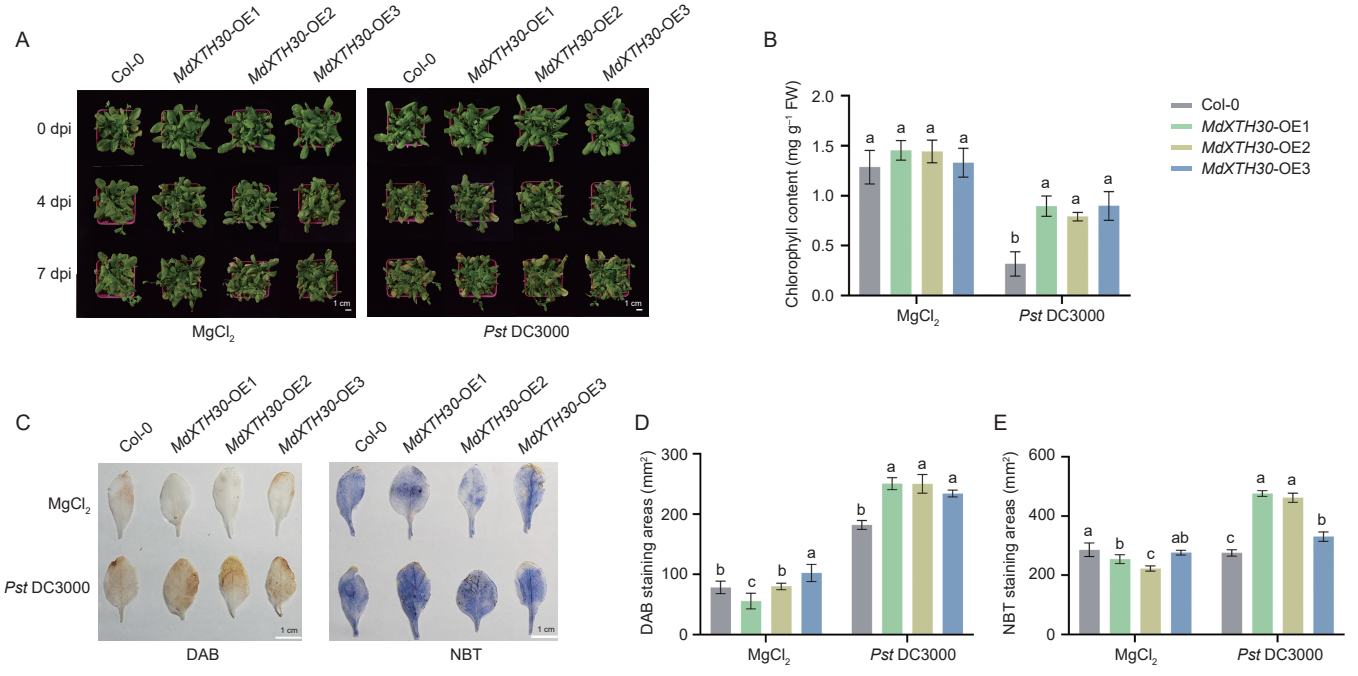


Fig. 10 *MdXTH30* enhances pathogenic bacteria resistance in *Arabidopsis*. A, phenotypes of *MdXTH30* transgenic *Arabidopsis* and Col-0 at 0, 4 and 7 d post inoculation (dpi) with $MgCl_2$ and *Pst* DC3000 (bar=1 cm). B, chlorophyll content. C, *MdXTH30* transgenic *Arabidopsis* and Col-0 were subjected to DAB and NBT staining following inoculation with $MgCl_2$ and *Pst* DC3000 (bar=1 cm). D, DAB staining area was measured using Image J software (bar=1 cm). E, NBT staining area was measured using Image J software (bar=1 cm). Values represent mean±SD of at least three biological replicates. Different lowercase letters indicate significant differences at $P<0.05$.

Biological implications for cell wall metabolism. *The Plant Cell*, **19**, 1947–1963.
Behar H, Graham S W, Brumer H. 2018. Comprehensive cross-genome survey and phylogeny of glycoside hydrolase family 16 members reveals the evolutionary origin of EG16 and XTH proteins in plant lineages. *The Plant Journal*, **95**, 1114–1128.
Bi H, Liu Z, Liu S, Qiao W, Zhang K, Zhao M, Wang D. 2024. Genome-wide analysis of wheat xyloglucan endotransglucosylase/hydrolase (XTH) gene family revealed *TaXTH17* involved in abiotic stress responses. *BMC Plant Biology*, **24**, 640.
Charng Y Y, Mitra S, Yu S J. 2022. Maintenance of abiotic stress memory in plants: Lessons learned from heat acclimation. *The Plant Cell*, **35**, 187–200.
Eklöf J M, Brumer H. 2010. The XTH gene family: An update on enzyme structure, function, and phylogeny in xyloglucan remodeling. *Plant Physiology*, **153**, 456–466.
Le Gall H, Philippe F, Domon J M, Gillet F, Pelloux J, Rayon C. 2015. Cell wall metabolism in response to abiotic stress. *Plants*, **4**, 112–166.
Gu K D, Zhang Q Y, Yu J Q, Wang J H, Zhang F J, Wang C K, Zhao Y W, Sun C H, You C X, Hu D G, Hao Y J. 2021. R2R3-MYB transcription factor *MdMYB73* confers increased resistance to the fungal pathogen *Botryosphaeria dothidea* in apples via the salicylic acid pathway. *Journal of Agricultural and Food Chemistry*, **69**, 447–458.
Han J, Liu Y, Shen Y, Li W. 2023. A Surprising diversity of xyloglucan endotransglucosylase/hydrolase in wheat: New in sight to the roles in drought tolerance. *International Journal of Molecular Sciences*, **24**, 9886.
Han Y, Han S, Ban Q, He Y, Jin M, Rao J. 2017. Overexpression of persimmon *DkXTH1* enhanced tolerance to abiotic stress and delayed fruit softening in transgenic plants. *Plant Cell Reports*, **36**, 583–596.
Han Y, Wang W, Sun J, Ding M, Zhao R, Deng S, Wang F, Hu Y, Wang Y, Lu Y, Du L, Hu Z, Diekmann H, Shen X, Polle A, Chen S. 2013. Populus euphratica XTH overexpression enhances salinity tolerance by the development of leaf succulence in transgenic tobacco plants. *Journal of Experimental Botany*, **64**, 4225–4238.
Henrissat B, Davies G. 1997. Structural and sequence-based classification of glycoside hydrolases. *Current Opinion in Structural Biology*, **7**, 637–644.
Hu D G, Ma Q J, Sun C H, Sun M H, You C X, Hao Y J. 2016. Overexpression of *MdSOS2L1*, a CIPK protein kinase, increases the antioxidant metabolites to enhance salt tolerance in apple and tomato. *Physiologia Plantarum*, **156**, 201–214.
Huang W N, Liu H K, Zhang H H, Chen Z, Guo Y D, Kang Y F. 2013. Ethylene-induced changes in lignification and cell wall-degrading enzymes in the roots of mungbean (*Vigna radiata*) sprouts. *Plant Physiology and Biochemistry*, **73**, 412–419.
Jiang Y, Li Y, Lu C, Tang Y, Jiang X, Gai Y. 2020. Isolation and characterization of *Populus xyloglucan* endotransglycosylase/hydrolase (XTH) involved in osmotic stress responses. *International Journal of Biological Macromolecules*, **155**, 1277–1287.
Li Q, Hu A, Dou W, Qi J, Long Q, Zou X, Lei T, Yao L, He Y, Chen S. 2019. Systematic analysis and functional validation of citrus XTH genes reveal the role of Csxth04 in citrus bacterial canker resistance and tolerance. *Frontiers in Plant Science*, **10**, 1109.
Li Q, Zhu P, Yu X, Xu J, Liu G. 2024. Physiological and molecular mechanisms of rice tolerance to salt and drought stress: Advances and future directions. *International Journal of Molecular Sciences*, **25**, 9404.
Liu Y J, An J P, Wang X F, Gao N, Wang X, Zhang S, Gao W S, Hao Y J, You C X. 2021. *MdBZR1* regulates ABA response by modulating the expression of *MdABI5* in apple. *Plant Cell Reports*, **40**, 1127–1139.
Ma M, Yuan Y, Cheng C, Zhang Y, Yang S. 2021. The gene is involved in fruit softening in 'Golden Del. Reinders'. *Journal of the Science of Food and Agriculture*, **101**, 564–572.
Ma Y S, Jie H D, Zhao L, Lv X Y, Liu X C, Tang Y Y, Zhang Y, He P L, Xing H C, Jie Y C. 2022. Identification of the xyloglucan endotransglycosylase/hydrolase (*XTH*) gene family members expressed in *Boehmeria nivea* in response to cadmium stress. *International Journal of Molecular Sciences*, **23**, 16104.
Muñoz-Bertomeu J, Miedes E, Lorences E P. 2013. Expression of xyloglucan endotransglucosylase/hydrolase (XTH) genes and XET activity in ethylene treated apple and tomato fruits. *Journal of Plant Physiology*, **170**, 1194–1201.
Ngou B P M, Ding P, Jones J D G. 2022. Thirty years of resistance: Zig-zag through the plant immune system. *The Plant Cell*, **34**, 1447–1478.
Otulak-Kozieł K, Kozieł E, Bujarski J J. 2018. Spatiotemporal changes in xylan–1/xyloglucan and xyloglucan xyloglucosyl transferase (XTH-Xet5) as a step-in of ultrastructural cell wall remodelling in potato–potato virus Y (PVYNTN) hypersensitive and susceptible reaction. *International Journal of Molecular Sciences*, **19**, 2287.
Rose J K C, Braam J, Fry S C, Nishitani K. 2002. The XTH Family of enzymes involved in xyloglucan endotransglucosylation and endohydrolysis: Current perspectives and a new unifying nomenclature. *Plant and Cell Physiology*, **43**, 1421–1435.
Tiika R J, Wei J, Cui G, Ma Y, Yang H, Duan H. 2021. Transcriptome-wide characterization and functional analysis of xyloglucan endo-transglycosylase/hydrolase (XTH) gene family of *Salicornia europaea* L. under salinity and drought stress. *BMC Plant Biology*, **21**, 491.
Tuang Z K, Wu Z, Jin Y, Wang Y, Oo P P Z, Zuo G, Shi H, Yang W. 2020. *Pst* DC3000 infection alleviates subsequent freezing and heat injury to host plants via a salicylic acid-dependent pathway in *Arabidopsis*. *Plant*, *Cell & Environment*, **43**, 801–817.
Wang J H, Sun Q, Ma C N, Wei M M, Wang C K, Zhao Y W, Wang W Y, Hu D G. 2024. *MdWRKY31-MdNAC7* regulatory network: Orchestrating fruit softening by modulating cell wall-modifying enzyme *MdXTH2* in response to ethylene signalling. *Plant Biotechnology Journal*, **22**, 3244–3261.
Wu Z, Cui C, Xing A, Xu X, Sun Y, Tian Z, Li X, Zhu J, Wang G, Wang Y. 2021. Identification and response analysis of xyloglucan endotransglycosylase/hydrolases (XTH) family to fluoride and aluminum treatment in *Camellia sinensis*. *BMC Genomics*, **22**, 761.
Xie Y H, Zhang F J, Sun P, Li Z Y, Zheng P F, Gu K D, Hao Y J, Zhang Z, You C X. 2022. Apple receptor-like kinase FERONIA regulates salt tolerance and ABA sensitivity in *Malus domestica*. *Journal of Plant Physiology*, **270**, 153616.
Yokoyama R, Rose J K C, Nishitani K. 2004. A surprising diversity and abundance of xyloglucan endotransglucosylase/hydrolases in rice. Classification and expression analysis. *Plant Physiology*, **134**, 1088–1099.
Zhai Z, Feng C, Wang Y, Sun Y, Peng X, Xiao Y, Zhang X, Zhou X, Jiao J, Wang W, Du B, Wang C, Liu Y, Li T. 2021. Genome-wide identification of the xyloglucan endotransglucosylase/hydrolase (XTH) and polygalacturonase (PG) genes and characterization of their role in fruit softening of sweet cherry. *International Journal of Molecular Sciences*, **22**, 12331.
Zhang B, Gao Y, Zhang L, Zhou Y. 2021. The plant cell wall: Biosynthesis, construction, and functions. *Journal of Integrative Plant Biology*, **63**, 251–272.
Zhang C L, Wang G L, Zhang Y L, Hu X, Zhou L J, You C X, Li Y Y, Hao Y J. 2021. Apple SUMO E3 ligase *MdSIZ1* facilitates SUMOylation of *MdARF8* to regulate lateral root formation. *New Phytologist*, **229**, 2206–2222.
Zhang Z, Wang N, Jiang S, Xu H, Wang Y, Wang C, Li M, Liu J, Qu C, Liu W, Wu S, Chen X, Chen X. 2017. Analysis of the xyloglucan endotransglucosylase/hydrolase gene family during apple fruit ripening and softening. *Journal of Agricultural and Food Chemistry*, **65**, 429–434.
Zhong M S, Jiang H, Cao Y, Wang Y X, You C X, Li Y Y, Hao Y J. 2020. *MdCER2* conferred to wax accumulation and increased drought tolerance in plants. *Plant Physiology Biochemistry*, **149**, 277–285.

Executive Editor-in-Chief Sanwen Huang
Managing Editor Lingyun Weng